

# PARTICLE SIMULATION OF DARHT-II DOWNSTREAM TRANSPORT

B. R. Poole, Y. -J. Chen, Y. J. (Judy) Chen, A. C. Paul, L. -F. Wang  
Lawrence Livermore National Laboratory, Livermore, CA 94550, USA

## Abstract

The DARHT-II beamline utilizes a fast stripline kicker to temporally chop a high current electron beam from a single induction LINAC and deliver multiple temporal electron beam pulses to an x-ray converter target. To obtain a high quality radiographic measurement requires that high beam quality be maintained throughout the transport line from the end of the accelerator through the final focus lens and to the x-ray converter target. Issues that will affect beam quality such as spot size and emittance at the converter target include dynamic effects associated with the stripline kicker as well as emittance growth due to the nonlinear forces associated with the kicker and various focusing elements in the transport line. A particle-in-cell code is utilized to evaluate beam transport in the downstream transport line in DARHT-II. External focusing forces are included utilizing either analytic expressions or field maps. From these simulations, for various initial beam loads based on expected accelerator performance the temporally integrated spot size and emittance can be estimated.

## 1 INTRODUCTION

High resolution x-ray radiography on the second axis of the Dual Axis Radiographic Hydrodynamic Test Facility (DARHT-II) requires that the high current, high energy (2 kA at 20 MeV) electron beam be focused to a small (~1 mm) time integrated spot on an x-ray converter target. The DARHT-II beamline has been discussed previously [1] and is shown in Figure 1. Four short current pulses with various lengths will be selected out of the 2  $\mu$ s long pulse from the accelerator using a fast kicker system [2], [3].

The post-accelerator transport system consists of four sections. The first, a solenoidal transport system consisting of several solenoids between the accelerator exit and the kicker system matches the beam from the accelerator exit to the kicker subsystem, or is used as a diagnostic to extract initial beam conditions by measuring the beam size using three different magnetic transport settings [4]. The second transport subsystem is the kicker system that directs the beam into either the dump beamline or the target beamline. Normally, a static bias dipole magnet is used to direct the beam into the dump beamline. The quadrupole septum magnet gives an additional dipole kick to the beam as well as a de-focusing force in the kick plane to reduce the energy density at the

beam dump. When the fast stripline kicker is energized, the effective kick from the bias dipole is cancelled by the dynamic dipole field associated with the kicker, and the beam is injected into the center of the quadrupole septum magnet where the beam experiences only quadrupole de-focusing in the kick plane. Three Collins' quadrupoles re-establish a round beam after the quadrupole septum magnet. Collins' quadrupoles are used due to severe space constraints in this region of the beamline. The kicker system also includes a static bias sextupole winding to cancel the inherent sextupole field component associated with the dynamic kicker fields. The sextupole bias field is required to minimize emittance growth in the kicker subsystem for most of the duration of the switched beam. More will be discussed about the kicker subsystem in the modelling section. The third section is the target beamline, which is comprised of a solenoidal transport channel and the final focus lens that is used to provide a small spot on the x-ray converter target. The fourth transport section is the dump beamline that consists of a dipole magnet to further bend the beam into the beam dump. Magnetic shielding consisting of several layers of highly permeable material is provided in the region between the target and dump beamlines to prevent magnetic field leakage from the dump line dipole magnet into the target beamline and degrading the performance of the target beamline. In this paper we discuss only the modelling of the first three transport sections; from the accelerator exit through the x-ray converter target; the dump beamline will not be discussed in this paper.

The DARHT-II beamline is initially modelled using the TRANSPORT code to construct the appropriate magnetic transport system. A typical TRANSPORT simulation showing the beam envelope for the kick plane, ( $x$ ) and the non-kick plane, ( $y$ ) from the accelerator exit to the x-ray converter target is shown in Figure 2. Particle simulations can provide additional information on the performance of the beamline. Nonlinear forces due to higher order multipoles in the various beamline elements, nonlinear space charge forces, and nonlinear image forces can provide information on the emittance growth in the beamline. The formation of beam halo and particle loss can be analysed using particle simulations. Typically, a K-V particle load based on the sigma matrix from a TRANSPORT simulation is used for the initial beam conditions but more complex beam loads may be used from the results of other simulation codes.

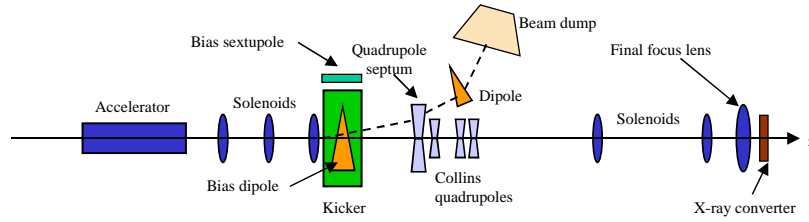


Figure 1: DARHT-II downstream transport line.

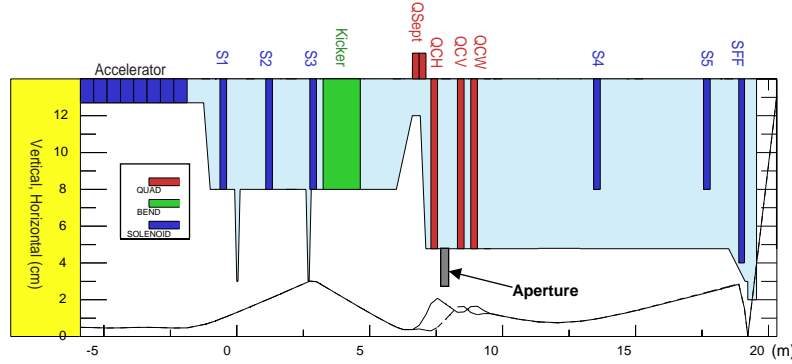


Figure 2: Transport simulation showing the DARHT-II beam envelope from the accelerator exit to the x-ray converter.

## 2 MODELLING

Multi-slice particle simulations are utilized to model the transport of a long pulse beam from the accelerator exit, through the kicker subsystem, and to the x-ray converter target. Analytic field distributions are typically used to describe the external fields for the various magnetic elements along the transport line. However, the kicker deserves a more detailed description.

The stripline kicker, shown schematically in Fig. 3 is designed to spatially separate an electron beam into two separate beamlines. A high voltage pulse is applied to the downstream ports of the kicker and the beam is kicked by the electric and magnetic fields associated with the TEM waves propagating on the strip transmission lines.

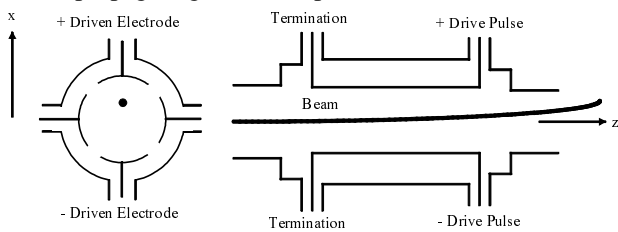


Figure 3: Schematic of fast beam kicker.

The potential within the kicker plates ( $r < b$ ) is given by Equation 1

$$V = \frac{4V_p}{\pi} \sum_{n=odd} \left( \frac{1}{n} \right) \sin\left(\frac{n\phi_0}{2}\right) \cos(n\phi) \left(\frac{r}{b}\right)^n \quad (1)$$

where  $b$  is the interior radius of the kicker plates,  $\phi_0$  is the angle subtended by each kicker plate, and  $V_p$  is the kicker plate voltage. The  $n = 1$  term in Eq. 1 represents the transverse dipole force that provides the beam steering

and terms with  $n \geq 3$  will contribute to the emittance growth in the structure.

The particle-in-cell (PIC) simulations for the DARHT-II beamline include beam corkscrew and energy variation within the beam pulse as well as temporal variation of the kicker TEM fields. Space charge, image forces and charge and current redistribution in particle slices are included in the simulations as well as tallying where particle loss occurs along the transport line.

Figure 4 shows the particle load of 2000 particles for a single slice of a nominal 20 MeV K-V beam with an unnormalized emittance of 3 cm-mr at the accelerator exit. The effect of the kicker sextupole field is shown in Fig. 5, which shows the transverse phase space 1 meter after the kicker with an emittance increase of 15%. The emittance growth can be effectively eliminated by the inclusion of a bias sextupole coil. Figure 6 shows a typical kicker voltage pulse and the resultant current at the target. The sharpened rise and fall time of the target current is caused by the scraping of particles as the beam is swept transversely by the kicker.

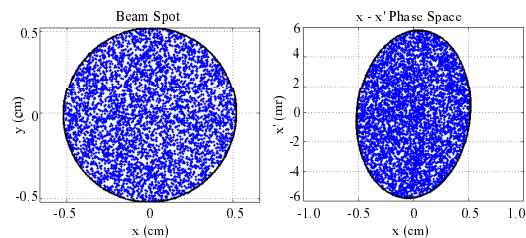


Figure 4: Initial transverse phase space at accelerator exit for a 20 MeV, 2 kA, 3 cm-mr beam

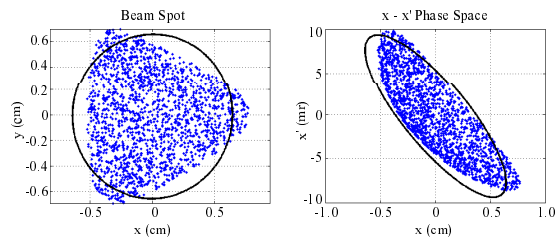


Figure 5: Effect of kicker sextupole field on transverse phase space in kick plane 1 meter after kicker exit

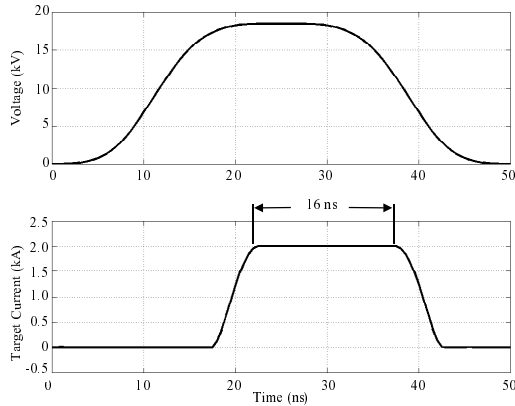


Figure 6: Kicker voltage waveform and target beam current showing pulse sharpening due to beam scraping.

Figure 7 shows the projections of the beam envelope in the  $x$ - $z$  and  $y$ - $z$  planes during the beam switch. The aperture is included to further sharpen the target current pulse.

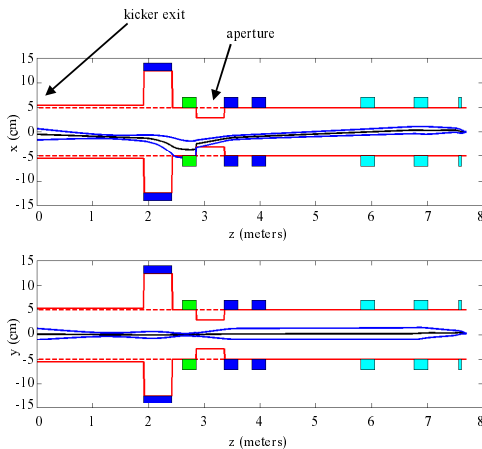


Figure 7: Beam envelopes during kicker switch time showing beam scraping at downstream aperture

An important figure of merit in the performance of DARHT-II is the time integrated spot size on the x-ray converter target. Figure 8 shows a cumulative or time-integrated phase space at the x-ray converter target allowing a bounding ellipse to provide an effective time

integrated spot size and emittance. The simulation utilized 200 slices over a 50 ns pulse. The spot has an extended size in  $y$  due to the combined effect of transverse motion during the kicker switch and the rotation of the elliptical spot due to the final focus solenoid.

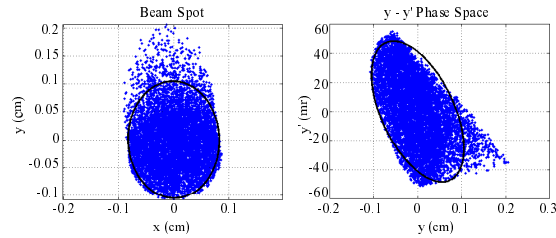


Figure 8: Time integrated target spot and phase space for 150 beam slices.

The effective spot size is 1.66 mm in  $x$  and 2.4 mm in  $y$  and the effective emittances are 3.28 cm-mr and 6.1 cm-mr in  $x$  and  $y$  respectively.

### 3 CONCLUSIONS

Multi-slice particle simulations provide significant information about the performance of a beamline by including a variety of physics models for transport components. Simulations for the DARHT-II beamline have been performed including beam corkscrew motion, energy variation, and kicker dynamical effects. Space charge, and image forces are also included in the analysis including effects due to charge and current redistribution along the beamline. Estimates of the temporal variation of spot size and emittance can be determined at the x-ray converter target and are useful in estimating dose.

### 4 ACKNOWLEDGEMENTS

Thanks go to Scott Nelson for help with the space charge algorithms in the PIC code. This work was performed under the auspices of the U.S. Department of Energy by the Lawrence Livermore National Laboratory under contract No. W-7405-ENG-48.

### REFERENCES

- [1] A.C. Paul, G. J. Caporaso, Y. -J. Chen, Y. J. (Judy) Chen, G. Westenskow, "The Beamline for the Second Axis of the Dual Axis Radiographic Hydrodynamic Test Facility", PAC'99, New York, March 1999.
- [2] B.R. Poole, G. J. Caporaso, Y. J. (Judy) Chen, L. -F. Wang, "Analysis and Modelling of a Stripline Beam Kicker and Septum", LINAC'98, Chicago, August 1998.
- [3] Y. J. (Judy) Chen, G. J. Caporaso, J. T. Weir, "Precision Fast Kickers for Kiloampere Electron Beams", PAC'99, New York, March 1999.
- [4] A.C. Paul, "Reconstruction of Initial Beam Conditions at the Exit of the DARHT-II Accelerator", LINAC'2000, Monterey, August 2000.